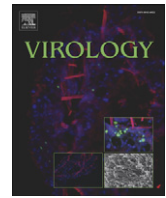




Contents lists available at SciVerse ScienceDirect

Virology

journal homepage: www.elsevier.com/locate/yviro

Functional regulation of PVBV Nuclear Inclusion protein-a protease activity upon interaction with Viral Protein genome-linked and phosphorylation

C. Mathur ^a, V.K. Jimsheena ^c, S. Banerjee ^b, K. Makinen ^d, L.R. Gowda ^c, H.S. Savithri ^{a,*}

^a Department of Biochemistry, Indian Institute of Science, Bangalore-560012, India

^b Molecular Biophysics Unit, Indian Institute of Science, Bangalore-560012, India

^c Department of Protein Chemistry and Technology, Central Food Technological Research Institute, Mysore-570020, India

^d Department of Food and Environmental Sciences, University of Helsinki, Helsinki-00014, Finland.

ARTICLE INFO

Article history:

Received 9 July 2011

Accepted 10 October 2011

Available online 17 November 2011

Keywords:

Potyviridae

Pepper Vein Banding Virus (PVBV)

Nuclear Inclusion protein-a protease (NIa-Pro)

Viral Protein genome-linked (VPg)

VPg-Pro

HPLC-based protease assay

Molecular modeling

ABSTRACT

Regulation of NIa-Pro is crucial for polyprotein processing and hence, for successful infection of potyviruses. We have examined two novel mechanisms that could regulate NIa-Pro activity. Firstly, the influence of VPg domain on the proteolytic activity of NIa-Pro was investigated. It was shown that the turnover number of the protease increases when these two domains interact (*cis*: two-fold; *trans*: seven-fold) with each other. Secondly, the protease activity of NIa-Pro could also be modulated by phosphorylation at Ser129. A mutation of this residue either to aspartate (phosphorylation-mimic) or alanine (phosphorylation-deficient) drastically reduces the protease activity. Based on these observations and molecular modeling studies, we propose that interaction with VPg as well as phosphorylation of Ser129 could relay a signal through Trp143 present at the protein surface to the active site pocket by subtle conformational changes, thus modulating protease activity of NIa-Pro.

© 2011 Elsevier Inc. All rights reserved.

Introduction

Pepper Vein Banding Virus (PVBV), a distinct member of the genus potyvirus (Family: *Potyviridae*), is a flexuous, non-enveloped, rod-shaped virus (Ravi et al., 1997). It has a 9.7 kb single-stranded positive sense RNA genome which encodes for an approximately 340 kDa polyprotein (Fig. 1A; Anindya et al., 2004). The potyviral genome is translated either as a polyprotein encoded by the open reading frame or as unique proteins resulting from ribosomal frameshifting / translational slippage (Chung et al., 2008; Riechmann et al., 1992; Urcuqui-Inchima et al., 2001; Wei et al., 2010; Wen and Hajimorad, 2010). The polyprotein is proteolytically processed by P1-protease (P1-pro), Helper Component-protease (HC-Pro) and Nuclear Inclusion protein-a protease (NIa-Pro), generating various intermediates and mature proteins at different stages of the viral life cycle (Urcuqui-Inchima et al., 2001). While P1-Pro and HC-Pro cleave at their own C-termini to release the respective domains from the polyprotein, NIa-Pro cleaves at seven sites within the polyprotein (Fig. 1A; Mavankal and Rhoads, 1991; Riechmann et al., 1992). The full length VPg-Pro has two domains; an N-terminal Viral Protein genome-linked (VPg) and a C-terminal protease (NIa-

Pro). The potyviral NIa-Pro is shown to be analogous to picornavirus 3C protease (Matthews et al., 1994). The recombinant proteases from potyviruses like PVBV, Tobacco Etch Virus (TEV) and Turnip Mosaic Virus (TuMV) have been shown to be active *in trans* (Anindya and Savithri, 2004; Joseph and Savithri, 2000; Kim et al., 2000; Riechmann et al., 1992). The crystal structures of the NIa-Pro domain from the TEV and Tobacco vein mottling virus (TVMV) have shown that the protease has an anti-parallel β -barrel fold, which is typical of chymotrypsin-like proteases (Phan et al., 2002; Sun et al., 2010). The catalytic triad is formed by a histidine, an aspartate and a cysteine (instead of a serine as in chymotrypsin) present at the active site (Dougherty and Semler, 1993; Joseph and Savithri, 2000; Riechmann et al., 1992). It recognizes a heptapeptide sequence between two protein domains, and cleaves at the C-terminus of a glutamine (P1 position in the recognition sequence), which is followed by a serine, threonine or alanine (P1' position). The recognition site between NIb and CP in PVBV is Gly(P7)-Gly(P6)-Glu(P5)-Val(P4)-Ala(P3)-His(P2)-Gln(P1)-Ala(P1'). The carboxy-terminal ~150 amino acid residues of the protease, which are least conserved among potyviruses, have been implicated to be involved in substrate binding by interacting with amino acid residues of the heptapeptide recognition sequence (Riechmann et al., 1992). The structural and kinetic data for proteases from TEV and TVMV demonstrate that the proteases are highly species-specific and are thus, much more efficient when cognate peptides are used as substrates. P3 and P4 positions within the

* Corresponding author. Fax: +91 80 2360 0814.

E-mail address: bchss@biochem.iisc.ernet.in (H.S. Savithri).

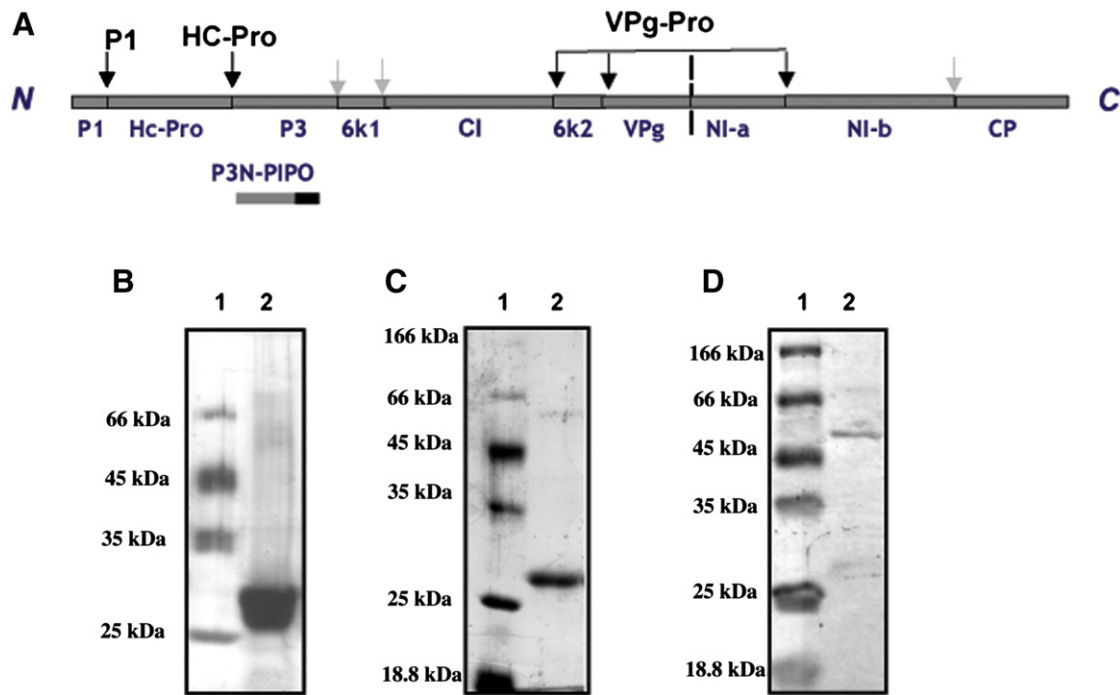


Fig. 1. (A) Domain organization of *Pepper Vein Banding Virus* polyprotein is shown and the individual domains released upon polyprotein processing are labeled below the schematic representation of the polyprotein. P3N-PIPO translated by ribosomal frameshift is also shown. P1, Hc-Pro and NIa-Pro mediated *cis*-cleavage (black arrows); NIa-Pro mediated *trans*-cleavage (gray arrows); sub-optimal cleavage site between NIa-Pro and VPg (dotted line) are shown. (B) SDS-PAGE analysis of Ni^{2+} -NTA purified NIa-Pro. Lane 1: molecular mass (kDa) markers, Lane 2: purified NIa-Pro. (C) SDS-PAGE analysis of Ni^{2+} -NTA purified VPg. Lane 1: molecular mass (kDa) markers, Lane 2: purified VPg. (D) SDS-PAGE analysis of Ni^{2+} -NTA purified E191A VPg-Pro. Lane 1: molecular mass (kDa) markers, Lane 2: purified E191A VPg-Pro.

heptapeptide sequence are shown to be crucial for conferring such stringent specificity to NIa-Pro (Phan et al., 2002; Sun et al., 2010; Tozser et al., 2005). NIa-Pro cleaves *in cis* at the junctions between CI/6K2, 6K2/VPg, VPg/Pro and Pro/NIb, and *in trans* at the junctions between P3/6K1, 6K1/CI and NIb/CP (Fig. 1A; Dougherty and Parks, 1991; Joseph and Savithri, 2000; Riechmann et al., 1992; Rorrer et al., 1992; Urcuqui-Inchima et al., 2001). The cleavage site between the VPg domain and the protease domain is suboptimal due to the presence of a glutamate instead of a glutamine at the P1 position. The slow processing at this site has been shown to be critical for viral replication, as an increase or a decrease in the cleavage rate at this position has debilitating effects on potyviral replication (Carrington et al., 1993; Schaad et al., 1996). Intermediate polypeptides that result from processing of a polyprotein by the proteases are known to play important roles in the life cycle of other viruses as well. For instance, in poliovirus, 3CD^{Pro}, the protease-replicase polyprotein intermediate, is important for complete processing of the capsids to yield mature virus particles (Harris et al., 1990; Palmenberg, 1990). The protease from *Sesbania Mosaic Virus* (SeMV), a sobemovirus, has been shown to be active *in cis* and *in trans*, only when VPg is fused to C-terminus of the protease (Satheshkumar et al., 2005). While the VPg of SeMV is a natively unfolded protein (Satheshkumar et al., 2005), the VPg domain of potyviral VPg-Pro is reported to be an internally disordered protein that may have some residual structure (Grzela et al., 2008; Hebrard et al., 2009; Rantalainen et al., 2008; Rantalainen et al., 2009). Potyviral VPg also undergoes phosphorylation *in vitro* and *in vivo* by host cell kinases, which may influence the translational processes and hence, viral assembly (Hafren and Makinen, 2008; Puustinen et al., 2002). VPgs from potyviruses and poliovirus are linked covalently to the respective viral genomes and are known to act as replication primers (Anindya et al., 2005; Ferrer-Orta et al., 2006; Murray and Barton, 2003; Paul et al., 1998; Puustinen and Makinen, 2004).

The internally disordered domains may act as the 'hub' for interaction with several proteins and thereby regulate their function

(Chouard, 2011). In this report, we show that the interaction of PVBV VPg and NIa-Pro influences the activity of the protease. Examination of the modeled structure of PVBV NIa-Pro revealed that the region containing Trp143 is most likely involved in interaction with VPg. Additionally, Ser129 of the protease domain was also shown to get phosphorylated by a soluble host cell kinase. Mutational analysis of these residues revealed that events occurring at the surface of the protease, such as interaction with VPg or phosphorylation at Ser129, can influence the orientation of residues present at the active site, and thus affect catalysis.

Results and discussion

Overexpression and purification of recombinant PVBV proteins

In order to examine the effect of VPg on the protease activity of NIa-Pro, VPg, NIa-Pro and VPg-Pro were expressed as N-terminal histidine-tagged proteins (His-VPg, His-NIa-Pro and His-VPg-Pro, respectively) in *E. coli* and purified as described in the Materials and methods section. The purified NIa-Pro migrated as two bands in SDS-PAGE (Fig. 1B, lane 2), one corresponding to the intact protein (~29 kDa) and another to a degradation product (~27 kDa). Mass spectrometric analysis of NIa-Pro confirmed that it tends to undergo slow degradation upon prolonged storage (data not shown).

Overexpression of VPg-Pro from pRVN clone in BL21 *E. coli* cells containing pSBET A yielded His-VPg and untagged NIa-Pro due to the cleavage between the two domains. SDS-PAGE analysis of purified histidine-tagged VPg showed a single band of ~27 kDa (Fig. 1C, lane 2) as against the calculated molecular mass of 23.6 kDa. This deviation in molecular mass could be due to high content of basic amino acid residues in the VPg primary sequence. The molecular size of histidine-tagged VPg (~23 kDa) was further confirmed by mass spectrometry (data not shown). Full length VPg-Pro (E191A VPg-Pro) was purified (Fig. 1D, lane 2) using the cleavage site mutant of VPg-Pro (pRVNE191A).

In vitro interaction of Nla-Pro and VPg

In order to examine plausible interaction between purified Nla-Pro and VPg domains, an ELISA-based assay was performed with some modifications to a protocol described earlier by Roy Chowdhury and Savithri (2011; and references therein). Direct antigen coating-ELISA (DAC-ELISA) was performed in wells coated with VPg to monitor its cross-reaction with anti-Nla-Pro primary antibodies (Fig. 2A, bar 2) and, in wells coated with Nla-Pro (Fig. 2A, bar 5), which served as a positive control. For testing interaction between Nla-Pro and VPg, ELISA plates were coated with ~0.2 nmol of VPg and the unoccupied sites were blocked. These plates were then incubated with ~0.2 nmol of Nla-Pro. Binding of Nla-Pro was detected using rabbit anti-Nla-Pro primary antibody, followed by HRP-conjugated goat anti-rabbit secondary antibody and 1× TMB/H₂O₂ substrate (Sub). The test modules (Fig. 2A, bar 6) showed a significantly higher absorbance at 450 nm when compared to the negative controls (Fig. 2A, bars 1–4). This indicated that Nla-Pro and VPg interact *in trans*. Furthermore, this interaction was confirmed by pull-down assays carried out using His-VPg and GST-Nla-Pro (Fig. S1). The interaction of VPg with Nla-Pro has also been reported earlier in *Soybean Mosaic Virus* (Kang et al., 2004) and *Potato Virus A* (PVA; Guo et al., 2001). The concentration dependence of the interaction between the two domains, determined using ~0.2 nmol of VPg and varying amount (0.06–0.34 nmol) of Nla-Pro, showed a linear correlation upto ~0.2 nmol of Nla-Pro (Fig. S2.), thus implying that the two domains may interact *in trans* with a stoichiometry of 1:1.

To gain insight into the nature of interaction between the two domains, the intrinsic fluorescence spectra for the recombinant proteins (Fig. 2B) were monitored by exciting the protein at 280 nm and recording the emission spectra from 300 to 400 nm. It is known that if a tryptophan residue is present at or near the ligand-binding site on a protein, then interaction with the ligand can cause quenching of tryptophan fluorescence (Freifelder, 1982). Nla-Pro has five tryptophans and two tyrosines, while the VPg domain has seven tyrosines,

but no tryptophans. Hence, while VPg (Fig. 2B, line 1) has a very low intrinsic fluorescence signal with an emission maximum at 335 nm, Nla-Pro (Fig. 2B, line 2) showed emission maxima in a broader range from 335 nm (corresponding to a folded protein with buried aromatic residues) to 352 nm (corresponding to exposed aromatic residues). In contrast, a distinct emission maximum was observed for E191A VPg-Pro (Fig. 2B, line 3) at 335 nm. Since VPg has no tryptophans, the spectrum for E191A VPg-Pro implicates burial of an exposed tryptophan residue due to interaction of the two domains. However, this spectrum may also reflect the altered folding of Nla-Pro when it is fused to VPg. Therefore in order to distinguish the effect of folding and interaction of the two domains on tryptophan fluorescence quenching, the intrinsic fluorescence was monitored when VPg was added *in trans* to Nla-Pro (Fig. 2B, line 4). In this spectrum, quenching of intrinsic fluorescence was observed especially around 350 nm, which further implied that certain tryptophan residues of Nla-Pro are probably present at the site of interaction between the two domains. Additionally, both these spectra were found to differ from the spectrum obtained by theoretical summation of Nla-Pro and VPg spectra (Fig. 2B, line 7), further substantiating the interaction between the two domains. Overall these studies demonstrate that the VPg and Nla-Pro domains interact with each other *in trans*, and possibly *in cis* as well, which may be important for regulating the activity of these two domains.

Comparative proteolytic activity profiles

In order to examine the effects of interaction between VPg and Nla-Pro on the functional properties of the protease, we developed a reverse phase-HPLC-based (RP-HPLC-based) protease assay for making quantitative estimations. A synthetic peptide with a sequence corresponding to that of the heptapeptide *trans* cleavage site between NIB and CP (Anindya et al., 2004; Joseph and Savithri, 2000; Parks et al., 1992) was used as a substrate for protease assays. At the N-terminus of the peptide (NH₂-WDGGEVAHQAGESV-COOH), a

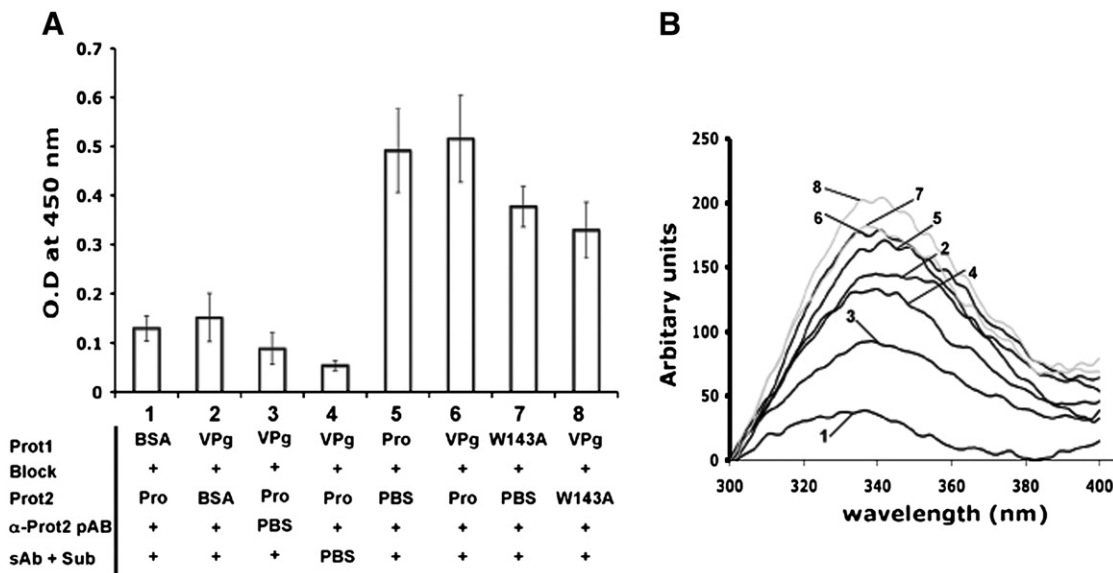


Fig. 2. Interaction of VPg and Nla-Pro. (A) ELISA-based interaction assay. VPg (Prot1)-coated ELISA modules were blocked by 5% BSA, followed by incubation with ~0.2 nmol of protease (Prot2; Pro = Wt Nla-Pro; W143A = W143A Nla-Pro), which was detected by incubation with rabbit anti-Nla-Pro primary antibody (α-Prot2 pAb), followed by goat anti-rabbit HRP conjugated secondary antibody (sAb) and 1X TMB/H₂O₂ as substrate (Sub). Bar 1: VPg (Prot1) negative control, Bar 2: Prot2 negative control, Bar 3: rabbit anti-Nla-Pro pAb negative control, Bar 4: sAb negative control, Bar 5: wild type Nla-Pro is used as Prot1 for direct antigen coating-ELISA as positive control, Bar 6: test for interaction between VPg (Prot1) and wild type Nla-Pro (Prot2), Bar 7: W143A Nla-Pro is used as Prot1 for direct antigen coating-ELISA as positive control, Bar 8: test for interaction between VPg (Prot1) and W143A Nla-Pro (Prot2). Details of steps are marked in the figure. Either BSA or PBS was added in negative control wells in place of proteins or antibodies, respectively. The bars represent the absorbance at 450 nm and standard deviations from three independent experiments are plotted as error bars. (B) Intrinsic fluorescence spectra were recorded for proteins (3.5 μM) in a buffer containing 25 mM Tris-HCl, pH 8.5 and 200 mM NaCl. The protein sample was excited at 280 nm and scanned for emission between 300 and 400 nm. (Line 1: VPg, Line 2: Nla-Pro, Line 3: E191A VPg-Pro, Line 4: VPg and Nla-Pro *in trans*, Line 5: W143A Nla-Pro, Line 6: VPg and W143A Nla-Pro *in trans*, Line 7: theoretical summation of intrinsic fluorescence of VPg and Nla-Pro, Line 8: theoretical summation of intrinsic fluorescence of VPg and W143A Nla-Pro.).

tryptophan was added (shown in bold) to aid monitoring of the cleavage reaction at 280 nm. Separation of substrate peptide as monitored at 220 nm and 280 nm, from the two expected products peptides, [NH₂-WDGGEVAHQ-COOH (P1) and NH₂-AGESV-COOH (P2)], is shown in Fig. 3A. The retention time of the purified substrate was 14.5 min, while that for purified product peptides, P1 and P2, were at 10.9 min and 3.6 min, respectively.

The wild type protease gets purified as two bands which vary in size by ~2 kDa (Fig. 1B). These two species were separated by gel-filtration and used in the protease assay. Both the species were found to have similar proteolytic activities (data not shown), as has been reported earlier for TuMV protease which undergoes autocatalytic cleavage to remove the C-terminal twenty amino acids from its protease. These residues are reportedly dispensable for cleavages at 6 K1-CI, Nla-NIb and NIb-CP junctions by TuMV protease (Kim et al., 1996, 1998). The representative RP-HPLC profile (Fig. 3B) of the assay reaction mixture using PVBV protease shows distinct separation of the substrate (Rt = 15.3 min), from the product peptide P1 (NH₂-WDGGEVAHQ-COOH; Rt = 12.1 min). The retention time for the product peptide P2 (NH₂-AGESV-COOH) was coincident with the buffer peak (Figs. 3 B and C). Protease assay carried out using an active site mutant (C151A) of Nla-Pro (Fig. 3C), did not show release of the product, indicating that the mutant enzyme was inactive. These results clearly showed that the PVBV Nla-Pro is capable of

cleaving the peptide substrate and, the RP-HPLC-based method of protease assay can be used for further characterization of the enzyme. Area under the curve for substrate and product peptide P1 was used for making quantitative estimations. The product release increased linearly with increasing Nla-Pro concentration and, with time upto ~100 min. The activity was found to be optimum in the presence of 1 mM MgCl₂, 1 mM DTT, 200 mM NaCl and 25 mM Tris-HCl, pH 8.5 (data not shown).

Using these assay conditions, the kinetic parameters, K_m and k_{cat} , for Nla-Pro were determined (Table 2). The effect of VPg, present *in trans* to Nla-Pro, on kinetic parameters of Nla-Pro protease activity (Table 2), was examined by a similar procedure. In E191A VPg-Pro, VPg domain is fused at the N-terminus of the Nla-Pro and could thus be used to examine the influence of *cis*-interaction of the two domains upon activity of Nla-Pro. As calculated using the Lineweaver-Burk plot, the K_m values for Nla-Pro and E191A VPg-Pro were found to be comparable. The K_m and k_{cat} values for Nla-Pro were found to be 0.44 mM and 0.034 s⁻¹, respectively. When VPg was present *in cis* with the protease, K_m was found to be 0.45 mM, while the k_{cat} nearly doubled to 0.063 s⁻¹. However, when VPg was added *in trans* to Nla-Pro in a 1:1 molar ratio, the K_m and k_{cat} values were found to be 1.67 mM and 0.23 s⁻¹, respectively. (The increase in K_m of the protease upon *trans* interaction of the two proteins could be attributed to residues corresponding to the Nla-Pro cleavage site

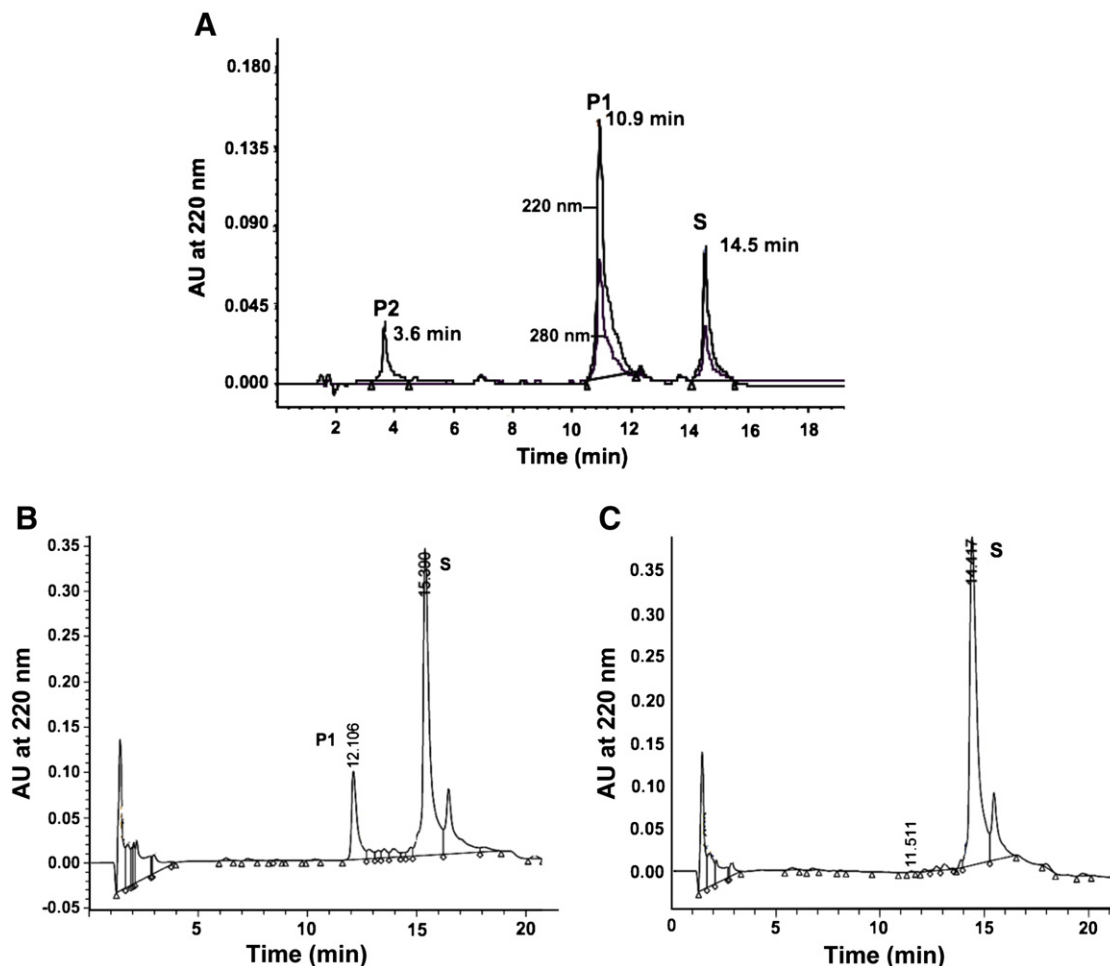


Fig. 3. RP-HPLC-based protease assay. The peptide substrate was synthesized by SPPS using standard Fmoc chemistry in an automated peptide synthesizer. (A) RP-HPLC profile for separation of purified substrate and product peptides using a C-18 column and gradient of 0.1% TFA (solvent A) and 70% acetonitrile in water containing 0.05% TFA (solvent B). Absorbance at 220 nm and 280 nm were monitored to identify substrate (S) and product (P1, P2) peaks. (B) The protease assay was performed with 2 μ M Nla-Pro in buffer containing 25 mM Tris-HCl, pH 8.5, 200 mM NaCl, 1 mM DTT, 1 mM MgCl₂ and 10% glycerol with 40 μ M peptide substrate. The reaction mixture was analyzed using RP-HPLC C18 column. Absorbance at 220 nm was monitored to identify substrate and product peaks. A representative figure for the RP-HPLC-based protease assay using the wild type Nla-Pro is shown and substrate (S) and product (P1) peaks are marked. (C) A representative figure for the protease assay using the active site mutant (C151A) of Nla-Pro is shown; substrate (S) peak is marked.

Table 1

Primers used for site-directed mutagenesis. The sequence marked in italics corresponds to the mutated residue, and the sequence marked in bold corresponds to the restriction site modified in the primer for screening.

Primer Name	Primer sequence (5'–3')	Restriction enzyme site
VN SEN	CG GGCTAG CGGATCCATGGCACAAAAGAAGAAACAAG	<i>NheI</i>
VN ANTI	TTCCATGGCTAGGATCCTTGCTCACGAACAAATGC	–
VN E191A SEN	GAAGGAG GTGCA CCATGCAGCCCGCTCG	<i>Sall</i>
VN E191A ANTI	CGAGCGGGCTGCATG GTGCA CTCCTTC	<i>Sall</i>
Nla S129A SEN	AGTCTTATTT CTGCAG ATGCCACAACATC	<i>PstI</i>
Nla S129A ANTI	TGATGTTGTGCAT CTGCAG AAATAAGAC	<i>PstI</i>
Nla S129D SEN	AGTCTTATTT CTGCAG ATGCCACAACATC	<i>PstI</i>
Nla S129D ANTI	TGATGTTGTGCAT CTGCAG AAATAAGAC	<i>PstI</i>
Nla W143 SEN	TTTTGGAGACACGG ATCGAT ACAAAGGATGGACAC	<i>Clal</i>
Nla W143 ANTI	CCATCCTTGC ATCGAT CGCGTGTCTCCAAAAC	<i>Clal</i>

present at the C-terminus of VPg, which may compete for binding at the protease active site.) Thus, VPg enhances the turnover number of the protease. The increase is more pronounced when the two domains are present *in trans* (seven-fold), as compared to when they are present *in cis* (two-fold). Such structural and functional modulation of Nla-Pro by differential interaction with VPg could be one of the important modes of regulation of the proteolytic activity at particular stages of virus life cycle.

We suggest that *cis* cleavages in the polyprotein may not require fast processing. The enzyme efficiency could be influenced by the proximity of the substrate and possible channeling of the cleavage sites into the active site pocket of the cognate Nla-Pro, in a manner similar to that of multi-enzyme complexes. However, once the protein intermediates are released from the polyprotein by *cis* cleavage, they would diffuse into the region surrounding the replication vesicles. It may be noted that the Nla-Pro catalytic activity in TEV has been reported to be diffusible (Carrington et al., 1993). Processing of these diffusible polyprotein intermediates may require an enzyme with a higher turnover number. We propose that VPg-supplemented Nla-Pro is more favorable than Nla-Pro for *trans* cleavage events, and VPg-Pro could be associated with *cis* cleavage of the PVBV polyprotein.

Sequence and structural analysis of PVBV Nla-Pro

In order to gain further insight into the Nla-Pro function and regulation, comparative sequence and structural analyses with homologous

Table 2

Kinetic parameters for the protease activity of recombinant wild type Nla-Pro of PVBV, and its variants or mutants, determined by RP-HPLC-based protease assay using synthetic peptide substrate. All experiments have been performed in triplicates, and the standard deviations are indicated wherever applicable.

	K_m (mM)	k_{cat} (per s)
1) Nla-Pro	0.44 ± 0.10	0.034 ± 0.008
2) E191A VPg-Pro	0.45 ± 0.14	0.063 ± 0.016
3) VPg <i>trans</i> Nla-Pro	1.67 ± 0.21	0.230 ± 0.022
4) W143A Nla-Pro	0.69 ± 0.05	0.002
5) W143A Nla-Pro + VPg	11.4 ± 3.2	0.01
6) S129D Nla-Pro	0.05 ± 0.02	0.004
7) VPg <i>trans</i> S129D Nla-Pro	0.15 ± 0.07	0.006
8) S129A Nla-Pro	0.06 ± 0.02	0.005

proteins were carried out. PVBV Nla-Pro shares sequence homology with 28 viral proteases deposited in the Swiss-Prot database, with sequence identities ranging from 35 to 50%. Among these proteins, TEV (PDB ID: 1LVM; Phan et al., 2002) and TVMV (PDB ID: 3MMG; Sun et al., 2010) have been structurally characterized and share a sequence identity of 47% and 45%, respectively, with PVBV Nla-Pro. In the absence of a crystal structure for PVBV Nla-Pro, a model of the protease was generated using the TEV Nla-Pro structure (PDB ID: 1LVM) as the template as described in Materials and Methods (Fig. 4A). As anticipated, PVBV Nla-Pro adopts a mixed two-domain anti-parallel β -barrel fold similar to those of chymotrypsin-like proteases. The catalytic triad was found to be conserved in PVBV Nla-Pro (His46, Asp81, Cys151), suggesting mechanistic similarity amongst these enzymes.

PVBV Nla-Pro contains five conserved tryptophans, of which only Trp143 is exposed to the solvent (Fig. 4A, orange), and is thus suitable for interaction with other molecules. Thus, quenching of intrinsic fluorescence at 350 nm observed upon interaction of VPg with Nla-Pro could be due to shielding of this residue (Fig. 2B). Trp143 lies on a loop that contains the active site cysteine (Cys151) of the protease (henceforth called W–C loop; H142–C151; Fig. 4A) and is reportedly involved in extensive interactions with the substrate as well as the products (Phan et al., 2002). Additionally, Trp143, His142, His167 and Cys151 are connected by a network of interactions (Fig. 4B). His142 is anchored by interactions with Ile144 and Phe179, while His167 is held by interaction with Thr146. Asn177 lies close to these histidines with its side-chain facing the W–C loop and interacting with the main-chain of Ile144. All these interacting residues (henceforth collectively called W–C region; Fig. 4B) are structurally conserved (Fig. S3) and were found to undergo correlated motion during molecular dynamics simulation carried out on the wild type PVBV Nla-Pro. Therefore, it appears that these residues could be important for relaying conformational changes that take place at the surface (Trp143) to the active site pocket (Cys151) upon binding of VPg with the protease, thereby altering its catalytic efficiency.

Analysis of Trp143A Nla-Pro mutant

To experimentally confirm the importance of Trp143 in Nla-Pro activity and regulation, W143A Nla-Pro was generated by site-directed mutagenesis, overexpressed and purified under conditions similar to those of the wild type protease. Interaction of W143A Nla-Pro with VPg was monitored by ELISA and fluorescence spectroscopy. As observed from the ELISA measurements, W143A Nla-Pro is competent to interact with the purified VPg domain (Fig. 2A, bar 8). The slightly lower signal in W143A Nla-Pro positive control (Fig. 2A, bar 7) indicates that the mutation has probably affected the conformation of one of the epitopes which might be a contributor to antigen–antibody interaction. The fluorescence spectrum for W143A Nla-Pro (Fig. 2B, line 5) showed that the peak at 350 nm was absent in the mutant, confirming that Trp143 is indeed an exposed aromatic residue which contributes to the signal at this wavelength. Moreover, unlike for the wild type protease, addition of VPg *in trans* to W143A Nla-Pro does not quench intrinsic fluorescence (Fig. 2B, line 6), although this spectrum differs from the theoretical summation (Fig. 2B, line 8) of individual spectra for the two proteins. This confirms that Trp143 is present at the interface of protease–VPg interaction.

Even though Trp143 lies at a distal surface from the active site (distance between Trp143 and Cys151 C α atoms: 14.47 Å), the mutation of this residue to alanine nearly abrogates the catalytic activity of the protease. W143A Nla-Pro (Table 2) was found to have a low turnover number (0.002 s⁻¹), while the K_m (0.69 mM) was closer to that of the wild type enzyme. This shows that W143A mutant could bind the substrate with equal affinity as that of the wild type protease, although it was unable to catalyze the cleavage reaction. Interestingly, addition of VPg *in trans* increases both the K_m

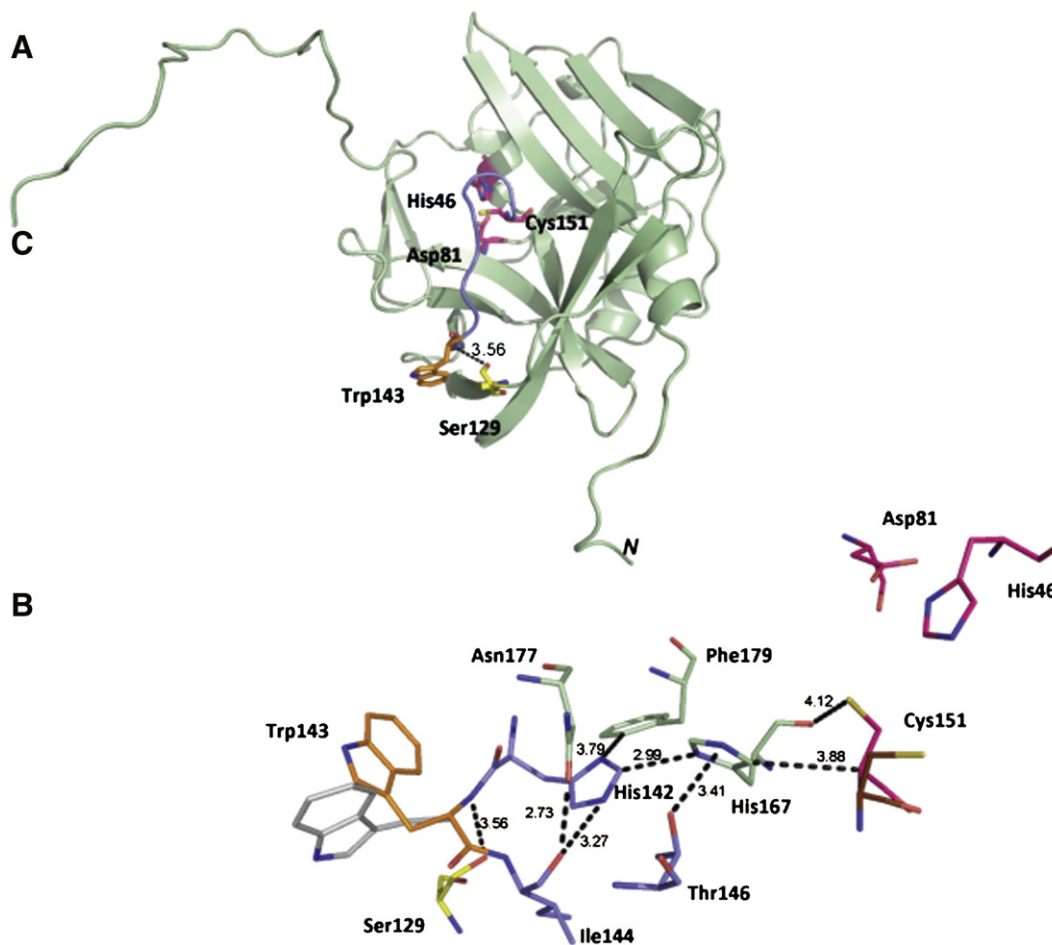


Fig. 4. (A) Structural model generated using LOMETS metaserver for PVBV Nla-Pro using TEV Nla-Pro structure as the template. Catalytic residues are marked in magenta, Ser129 in yellow, Trp143 in orange, W-C loop in blue. N- and C-termini of the protein are marked. Hydrogen bond between Trp143 and Ser129 is shown as dotted black lines. (B) Interaction network of W-C region. Catalytic residues (His46, Asp81, Cys151; magenta), Ser129 (yellow), Trp143 (orange), W-C loop residues (His142, Ile44, Thr146; blue), His 167 (green), Asn 177 (green), Phe179 (green) are marked. Snapshot of Cys151 (brown) of S129D Nla-Pro and Trp143 (gray) of S129A Nla-Pro from representative molecular dynamics simulations are superimposed. Distances are depicted as dotted black lines.

and k_{cat} of the mutant enzyme to 11.4 mM and 0.01 s^{-1} (Table 2), respectively.

Overall these results suggest that in the wild type protease, Trp143 could be important for maintaining the structural integrity of the W-C loop, and thus for protease activity. VPg most likely has multiple interactions with Nla-Pro at the face containing Trp143. These interactions may influence the residues of the W-C region and thus, regulate the activity of the protease upon binding to VPg.

Phosphorylation of VPg-Pro and the individual domains

Many stages in viral life cycle, such as assembly and disassembly, are modulated by phosphorylation (Ivanov et al., 2001, 2003), and a similar mechanism has been reported to affect the activity of PVA VPg (Hafren and Makinen, 2008; Puustinen et al., 2002). In order to determine if the protease domain of PVBV VPg-Pro undergoes phosphorylation, *in vitro* kinase assay was performed using the soluble fraction of the extract from leaves of *Nicotiana benthamiana* as the kinase source. Interestingly, the Nla-Pro domain was observed to get phosphorylated upon incubation with *N. benthamiana* plant extract in the presence of $[\gamma\text{-}^{32}\text{P}]\text{ATP}$ (Fig. 5A, lane 2), and the protein could undergo dephosphorylation upon treatment with a calf intestinal alkaline phosphatase (data not shown). Also PVBV VPg domain was observed to undergo phosphorylation (Fig. 5B) under similar assay conditions. However, a faint radioactive signal was found associated with E191A VPg-Pro in the absence (Fig. 5A, lane 5) and

presence (Fig. 5A, lane 4) of the kinase source suggesting that the full-length VPg-Pro does not get phosphorylated. A similar faint signal was also seen upon incubation of Nla-Pro with the radiolabel in the absence of the plant extract (Fig. 5A, lane 3). This signal could be due to non-specific binding of nucleotides to Nla-Pro and E191A VPg-Pro. These results imply that both Nla-Pro and VPg can be phosphorylated individually, but when the two protein domains interact *in cis* the phosphorylation sites of both the domains are masked, and thus, phosphorylation is not observed when E191A VPg-Pro is used as a substrate in the kinase assay.

Netphos analysis (Blom et al., 1999) carried out using Nla-Pro amino acid sequence predicted four amino acids, all of which were serine residues (Ser129, Ser132, Ser135 and Ser201) with high probability for phosphorylation. To experimentally determine the amino acid residue in the Nla-Pro sequence which gets phosphorylated, phosphoamino acid analysis was carried out by partial acid hydrolysis as described in the Materials and methods section. The acid hydrolysates were analyzed using thin layer chromatography. Fig. 5C (lanes 1–3) shows the relative mobilities of ninhydrin-stained phosphoserine, phospho-threonine and phospho-tyrosine, used as standards. The protein hydrolysate (Fig. 5C, lane 4) shows the appearance of two ninhydrin-stained spots. These two spots were also observed when the TLC sheet was exposed to phosphoimager (Fig. 5C, right panel). The mobility of the lower spot corresponds to a serine residue, indicating that at least one of the serine residues in the Nla-Pro sequence was phosphorylated by *N. benthamiana* cellular kinases. The

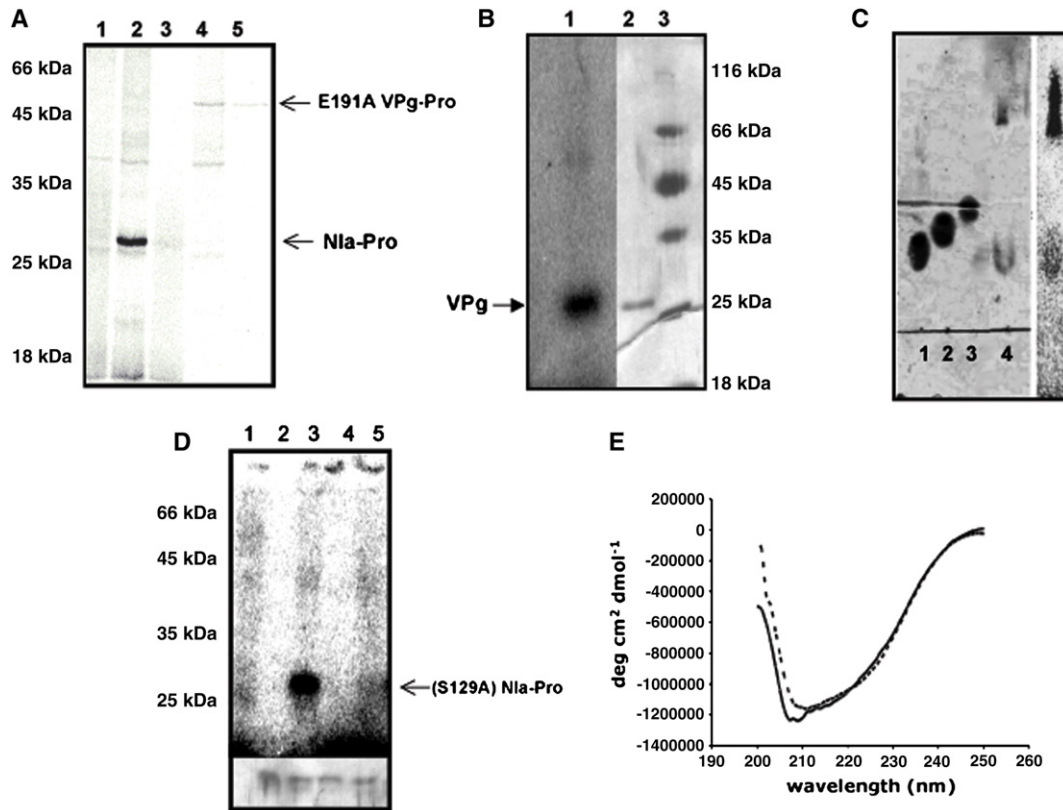


Fig. 5. (A) Phosphorylation of proteases. *In vitro* kinase assay was carried out using [γ -³²P]ATP as phosphoryl donor and assay mixtures were analyzed on SDS-PAGE, followed by phosphorimager analysis. Only plant extract without test protein was used as a negative control (lane 1). Phosphorimager analysis of *in vitro* kinase assay for Nla-Pro with (lane 2) and without (lane 3) *N. benthamiana* crude extract as the kinase source, and for E191A VPg-Pro with (lane 4) and without (lane 5) the plant extract are shown. (B) Phosphorylation of VPg. Lane 1: Phosphorimager analysis of *in vitro* kinase assay for VPg, lane 2: silver-stained gel for purified VPg; lane 3: protein molecular weight markers. (C) Phosphoamino acid analysis. Thin layer chromatogram of hydrolysates generated by *in gel* partial hydrolysis of phosphorylated Nla-Pro upon treatment with 6 N HCl at 110 °C for 2 h. Samples were spotted on cellulose TLC plates and developed using n-butyl alcohol, pyridine, acetic acid, water (15:10:13:2) as the solvent system. Ninhydrin-stained phospho-serine (lane 1), phospho-threonine (lane 2), phospho-tyrosine (lane 3) and Nla-Pro hydrolysate (lane 4) are shown. The Nla-Pro hydrolysate upon exposure to phosphorimager is shown in the right panel. (D) Phosphorylation of Nla-Pro mutant. Only plant extract without test protein was used as a negative control (lane 1). Phosphorimager analysis of *in vitro* kinase assay for Nla-Pro without (lane 2) and with (lane 3) *N. benthamiana* crude extract as the kinase source, and for S129A Nla-Pro without (lane 4) and with (lane 5) the plant extract are shown. Corresponding silver-stained SDS-PAGE is shown below the radiogram as loading control. (E) CD profile for wild type Nla-Pro (solid line) and S129D Nla-Pro (dotted line) far-UV range (200 to 250 nm) were recorded at a protein concentration of 1 mg/ml.

spot that moved further up could correspond to smaller peptides released due to incomplete hydrolysis of the protein.

One of the phosphorylation sites in the Nla-Pro sequence, predicted by the NetPhos analysis, was a serine at the position 129 (with respect to PVBV protease sequence). This is the only residue amongst the four predicted candidates which is conserved across potyviruses. Ser129 was found to be present on a surface-exposed loop in the modeled structure of PVBV Nla-Pro (Fig. 4A). In order to determine if Ser129 is one of the phosphorylated residues in Nla-Pro, it was mutated to alanine by site-directed mutagenesis, overexpressed and purified under conditions similar to those of the wild type Nla-Pro. In the *in vitro* kinase assay, phosphorylation of S129A Nla-Pro was drastically reduced (Fig. 5D, lanes 4–5) as compared to the wild type Nla-Pro (Fig. 5D, lanes 2–3). This suggested that Ser129 in Nla-Pro sequence undergoes phosphorylation by *N. benthamiana* cellular kinase.

Effect of phosphorylation on the proteolytic activity of Nla-Pro

It was of interest to examine the effect of phosphorylation of Ser129 on the protease activity of Nla-Pro. *In vitro* phosphorylation of Nla-Pro leads to phosphorylation of a small fraction of Nla-Pro, giving rise to a heterogeneous mixture of phosphorylated and unphosphorylated forms. In order to examine the influence of phosphorylation of Nla-Pro at Ser129 upon its structural and catalytic properties, a homogenous population of phosphorylated protein was required, and therefore an

alternative strategy was adopted. Negatively charged residues such as aspartate or glutamate have been reported to mimic the phosphorylated state of a protein (Leger et al., 1997). Ser129 of Nla-Pro was therefore mutated to aspartate by site-directed mutagenesis, and the mutant protein was purified under conditions similar to those of the wild type Nla-Pro. CD spectrum of S129D Nla-Pro showed only slight perturbations in the secondary structure as compared to the wild type enzyme (Fig. 5E).

The HPLC-based protease assay was employed to determine the kinetic parameters of Ser129 mutants of Nla-Pro (Table 2). K_m of S129D Nla-Pro, as determined from the Lineweaver–Burk plot, was found to be 0.05 mM, and the k_{cat} was found to be 0.004 s^{-1} . Addition of VPg *in trans* to the mutant did not enhance the activity of the enzyme significantly. Interestingly, the kinetic parameters for S129A Nla-Pro were found to be very similar to S129D Nla-Pro enzyme. The K_m for the S129A Nla-Pro was 0.06 mM, while the k_{cat} of S129A Nla-Pro (0.005 s^{-1}) was reduced by ten-fold when compared to wild type Nla-Pro, and by nearly a hundred fold as compared to VPg-supplemented Nla-Pro.

These studies suggest that Ser129 is another residue which is essential for the catalytic activity of Nla-Pro, even though it is present at a distal surface with respect to the active site (distance between Ser129 and Cys151 C α atoms: 16.9 Å). Interestingly, in the PVBV Nla-Pro model (Fig. 4A), Ser129 lies in close proximity to the surface-exposed Trp143. This provides additional support for the interaction between the two domains, which not only quenches tryptophan fluorescence when the two domains interact, but also masks the

site of phosphorylation on both the domains. Additionally, Ser129 lies on the most flexible region in the protease structure (Phan et al., 2002; Sun et al., 2010), and Trp143 lies on the flexible W–C loop. The side chain hydroxyl group of Ser129 could form a hydrogen bond with the main chain –NH group next to Trp143 (Fig. 4A). Mutation of Ser129 to either alanine, or possibly even aspartate, could disrupt or reorient this hydrogen bond and alter the conformation of the residues in the W–C region. Therefore, although it is unlikely that Ser129 is directly involved in catalysis, yet any mutation to this residue was not tolerated.

To understand the influence of phosphorylation of Ser129 *in silico*, the structural models for the phosphorylation-mimic S129D Nla-Pro and phosphorylation-deficient S129A Nla-Pro were also generated. Molecular dynamics simulations were carried out using GROMACS (Hess et al., 2008) for 30 ns for the structural models of wild type as well as mutant proteases. Superposition of snapshots at intervals of 500 ps illustrate that in S129A Nla-Pro, wherein the hydrogen bond between Ser129 and Trp143 is absent, the orientation of Trp143 was highly distorted as compared to the wild type protease (Fig. 4B). This implies that this hydrogen bond is crucial for maintaining Trp143 orientation and thus, protease function. Analysis of simulations for S129D Nla-Pro show that the catalytic Cys151 flips and faces away from the active site pocket (Fig. 4B), which might account for the loss of activity observed for the S129D mutant of Nla-Pro. The altered hydrogen bond between Ser129 and Trp143, and the change in orientation and movement of the W–C loop in S129D Nla-Pro, could perturb the residues in the W–C region causing the flip of Cys151, resulting in loss of activity. Interestingly, the turnover number of S129D Nla-Pro was not restored when it was supplemented with VPg *in trans*, unlike in W143A Nla-Pro. Therefore, it is likely that the interaction between Ser129 and Trp143 is crucial for protease activity as well as its regulation by VPg or phosphorylation, mediated via the residues present in the W–C region.

It has been previously suggested that polyprotein processing in potyviruses is closely regulated. The activity of Nla-Pro has been suggested to be modulated by three major mechanisms. Firstly, the sequence at the heptapeptide recognition site contains inherent information for a regulated cleavage (Dougherty and Parks, 1989), however, the local context of the cleavage site could also play an important role (García et al., 1992; Parks et al., 1992). Secondly, the recruitment of VPg-Pro into the nucleus to form inclusion bodies reduces the cytoplasmic concentration of the available protease (Riechmann et al., 1992). In the nucleus, VPg-Pro is speculated to interfere with host defenses and support infection (Anindya and Savithri, 2004; Beauchemin et al., 2007; Rajamaki and Valkonen, 2009; Restrepo et al., 1990). Thirdly, for some potyviruses, Nla-Pro could also be regulated by an internal cleavage at a non-canonical site near the C-terminus of Nla-Pro (Riechmann et al., 1992).

The results presented in the current study describe other possible mechanisms for regulation of PVBV Nla-Pro. Nla-Pro is known to occur in various forms, such as intermediate 6K2-VPg-Pro and VPg-Pro or, the mature Nla-Pro, as a result of temporally-controlled polyprotein processing. We have proposed that the interaction of Nla-Pro with VPg (especially *in trans*) significantly enhances protease activity via structural changes in the Trp143-containing loop (W–C loop). An earlier report by Parks et al. (1992) suggests that the cleavage site between TEV Nla-Pro is processed with nearly same efficiency by various protease intermediates, which supports our observation that the activity is minimally enhanced when VPg domain is present *in cis* with the protease domain. Therefore, although the cleavage site between Nla-Pro and VPg is sub-optimal, yet its cleavage could be essential in promoting *trans* interaction between the two domains. This could be crucial when high concentration of coat protein is required for nucleic acid encapsidation during viral morphogenesis.

We have also demonstrated for the first time that Nla-Pro undergoes phosphorylation at Ser129 which could cause subtle

structural changes in the protease and provide an important mechanism for the regulation of its activity. The phosphorylation and subsequent inactivation of Nla-Pro by the host cell kinases could thus be an important defense mechanism used by the plants to counteract PVBV infection.

Materials and methods

Cloning, overexpression and purification of proteins

The 1.3 kb VPg-Pro gene segment was amplified using primers mentioned in Table 1 and cloned between NheI and PvuII sites of pRSET C (Invitrogen) (pRVN) and the recombinant clone was confirmed by sequencing. Expression of pRVN in BL21 *E. coli* cells containing pSBET A, which enhances the rate of translation at the rare arginine codons, yielded His-VPg and untagged Nla-Pro due to cleavage between the domains by the protease. Thus, His-VPg-Pro was over-expressed in 1 l culture which was incubated for 4 h at 37 °C, induced using 0.3 mM IPTG and further grown for 12 h at 15 °C. For protein purification, the cells were harvested and lysed using a French press in resuspension buffer containing buffer R (10 mM CAPS-NaOH, pH 9.2, 200 mM NaCl) and 0.1% Nonidet P-40. Debris was removed by centrifugation and the supernatant was allowed to bind Ni²⁺-NTA resin for 2 h at 4 °C. The resin was packed into a column and washed with 100 ml wash buffer containing buffer R and 40 mM imidazole. Histidine-tagged VPg which remained bound to the resin was eluted in a buffer containing buffer R and 250 mM imidazole, dialyzed to remove imidazole and stored in buffer supplemented with 10% glycerol. Full-length VPg-Pro was expressed from the cleavage site mutant clone of VPg-Pro (pRVNE191A), under conditions similar to those described above. pRNIA clone (Anindya and Savithri, 2004) was cleaved with NheI and re-ligated to remove the extra residues added from the vector. This clone (pRNla-Pro) was used for His-Nla-Pro expression. The pRNla-Pro, active site C151A mutant (Joseph and Savithri, 2000), and other mutants (S129D, S129A, W143A) were transformed into BL21 pLysS *E. coli* cells, overexpressed and purified using the protocol described earlier (Anindya and Savithri, 2004) with a modification in the wash buffer composition (40 mM imidazole was used). Protein concentrations were determined using Lowry's method of protein estimation. ~3 mg His-Nla-Pro, ~1.5 mg His-VPg and ~0.25 mg His-E191A VPg-Pro was obtained from respective one liter cultures.

Site-directed mutagenesis

Site-directed mutagenesis (Weiner et al., 1994) was carried out using custom-made (Sigma) mutagenic DNA primers (Table 1) which were designed to mutate glutamic acid 191 to alanine in VPg-Pro to abolish the cleavage site between VPg and Nla-Pro domains. In Nla-Pro, serine 129 was mutated to alanine or aspartate, and tryptophan 143 was mutated to alanine. Presence of the desired mutations was screened by gain or loss of a restriction site and was confirmed by DNA sequencing.

ELISA-based protein interaction assay

ELISA modules (Nunc Axisorp F96F) were coated with ~0.2 nmol of VPg (200 µl) for 2 h. The plate was washed thrice with PBST (phosphate saline buffer, pH 7.5, with 0.1% Tween-20) and thrice with PBS for 3 min each. Unoccupied sites were blocked over-night using 350 µl of 5% bovine serum albumin (BSA; Bio-Rad), and the plate was washed four times with PBST and thrice with PBS for 3 min each. ~0.2 nmol of either Nla-Pro or W143A Nla-Pro was added to the plates, incubated for 1 h, and subjected to three washes with PBST and PBS each. Rabbit anti-Nla-Pro primary antibody (1:5000 dilution) was added to each well, incubated for 1 h, and washed as

before. HRP-conjugated goat anti-rabbit secondary antibody (1:10,000 dilution) was added to each well, incubated for 45 min and washed as before. 100 μ l substrate (1X TMB/H₂O₂) was added to each well. Reaction was stopped by the addition of 50 μ l of 2 M HCl and absorbance at 450 nm was measured using a Spectramax 340PC384 plate reader (Molecular Devices, Inc.). All dilutions were made in 1 \times PBS. For negative controls, BSA was added instead of the proteins and PBS instead of the antibodies. For positive controls, direct antigen coating-ELISA was performed using plates coated with 0.17 nmol Nla-Pro or W143A Nla-Pro prior to blocking. Antibody dilutions and incubation times were similar to the test experiments.

Fluorescence spectrophotometry

The intrinsic fluorescence was measured using a fluorescence spectrophotometer (Perkin-Elmer). Spectra were recorded at a protein concentration of 3.5 μ M in a buffer containing 25 mM Tris-HCl, pH 8.5 and 200 mM NaCl. The excitation wavelength was 280 nm and the emission was scanned between 300 and 400 nm.

Fmoc solid phase peptides synthesis (Fmoc-SPPS)

The peptides were assembled on an automatic peptide synthesizer (Model CS 136, CS Bio Co. San Carlos, CA) using standard Fmoc (Fmoc (N-(9-fluorenyl)methoxycarbonyl) chemistry (Merrifield, 1997). The peptides Trp-Asp-Gly-Gly-Glu-Val-Ala-His-Gln-Ala-Gly-Glu-Ser-Val, Trp-Asp-Gly-Gly-Glu-Val-Ala-His-Gln, and Ala-Gly-Glu-Ser-Val were synthesized using Wang resins pre-loaded with C-terminal glutamine or valine, having a substitution level of 0.6 meq/g or 0.31 meq/g (grain size-100–200 mesh), respectively. The peptides were obtained after cleavage from the peptidyl-resin and removal of side chain protecting groups using TFA/ethanedithiol/water/phenol/thioanisole (8:0.25:0.5:0.75:0.5, v/v), for 3 h at 25 $^{\circ}$ C, and purified by semi-preparative HPLC using a Shimadzu HPLC on a C-18 Shimpak column (25 cm \times 21.2 mm (i.d.), 10 M) and a binary gradient of 0.1% TFA (solvent A) and 70% acetonitrile in water containing 0.05% TFA (solvent B) at a flow rate of 15 ml/min from 0% to 100% buffer B in 60 min, and monitored at 220 nm. The sequences of the synthesized peptides were verified by amino acid analysis and N-terminal sequencing.

HPLC-based protease assay

The proteolytic activities for the Nla-Pro and C151A Nla-Pro (2 μ M) were assayed in buffer containing 25 mM Tris-HCl, pH 8.5, 200 mM NaCl, 1 mM DTT, 1 mM MgCl₂ and 10% glycerol with 40 μ M of the substrate (Trp-Asp-Gly-Gly-Glu-Val-Ala-His-Gln-Ala-Gly-Glu-Ser-Val) in a reaction volume of 50 μ l, incubated for 60 min at 25 $^{\circ}$ C and stopped by adding an equal volume of 0.2% trifluoroacetic acid (TFA), and centrifuging at 10,000 rpm for 10 min. Product peptides (Trp-Asp-Gly-Gly-Glu-Val-Ala-His-Gln, and Ala-Gly-Glu-Ser-Val) were separated from the substrate by RP-HPLC on a C18 column (Waters; 4.6 mm \times 25 cm) with a linear gradient of solvents A and B from 0% to 35% solvent B in 20 min at a flow rate of 1 ml/min and, detected at 220 nm and 280 nm. The area under the peak was measured and fractional cleavage was used to estimate the released product. Substrate concentration dependence was carried out using the same protocol with the peptide concentration varying from 0.014 mM to 1.4 mM. (Protein amounts used: Nla-Pro and mutants: 2.64 μ g, E191A VPg-Pro: 3.18 μ g). Using activity measurements determined in three independent experiments, K_m and k_{cat} values were estimated from the Lineweaver-Burk plot.

In vitro kinase assay

Plant sap was prepared by grinding lower leaves from three-week old *N. benthamiana* in buffer containing 25 mM HEPES, pH 7.4, 10%

sucrose and protease inhibitor cocktail (Sigma), and centrifuging at 10,000 rpm for 10 min, and used as the kinase source in the phosphorylation assay. The assay mixture had 25 mM HEPES, pH 7.4, 2 mM MnCl₂, and 2 μ Ci [γ -³²P]ATP (phosphoryl donor), along with 2 μ g protein and/or 2.5 μ g plant sap protein. It was incubated at 25 $^{\circ}$ C for 30 min and the reaction was stopped by boiling with SDS-PAGE loading buffer for 5 min. Phosphorylation of the proteins was monitored by analyzing the reactions on SDS-PAGE, followed by silver staining the gel and, exposing it to phosphorimager. Phosphorylation of purified PVA VPg was used as the positive control to determine the optimal assay conditions.

Thin layer chromatography

Proteins were subjected to *in vitro* phosphorylation using [γ -³²P]ATP and separated on SDS-PAGE. The protein band was excised and crushed gel pieces were subjected to partial *in gel* acid hydrolysis with 6 N HCl at 110 $^{\circ}$ C for 2 h. The volume was reduced to 2–3 μ l *in vacuo*. The hydrolysates were then analyzed by thin layer chromatography on cellulose plates (Merck). TLC chamber was equilibrated with buffer containing n-butyl alcohol, pyridine, acetic acid and water (15:10:13:2, v/v). 1 μ l of acid hydrolysates was spotted on TLC plates, along with phospho-serine, phospho-threonine and phospho-tyrosine as standards. The chromatogram was developed in the saturated chromatographic chamber, treated with ninhydrin and analyzed using a phosphorimager.

Circular dichroism spectroscopy

Circular dichroism (CD) spectra were recorded with a spectropolarimeter (Jasco J-715) equipped with a Peltier-type temperature controller (Jasco model PTC-348WI). A cuvette with 0.1 cm path-length and a protein concentration of 1 mg/ml in 25 mM Tris-HCl, pH 8.5 and 200 mM NaCl were used for all spectral measurements; bandwidth was 2 nm and three scans were recorded for each measurement with a scan speed of 10 nm/s. Background signal obtained in the absence of the protease was subtracted and the mean residue molar ellipticity, in units of deg.cm².dmol⁻¹, was determined from the corrected spectrum.

Homology modeling and molecular dynamics simulations

As attempts made to determine the crystal structure of the PVBV protease have not been successful, the amino acid sequences of Nla-Pro, S129A Nla-Pro and S129D Nla-Pro were submitted to LOMETS metaserver (Wu and Zhang, 2007) for homology modeling. The server generated multiple models of which those generated by HHSEARCH and SP3 algorithms using TEV and TVMV Nla-Pro as templates, respectively, were considered for further analysis. The two models thus generated, superposed 221 C-alpha atoms with a root mean square deviation (RMSD) of 0.93 \AA . PVBV Nla-Pro amino acid sequence shares 47% identity with TEV protease and, 45% identity with TVMV protease. The model generated using the TEV crystal structure was ranked as the best model and was found to have acceptable geometrical features, when evaluated using PROCHECK (Laskowski et al., 1993). About 98% of the residues lie in allowed regions of the Ramachandran plot. Thus, this particular model was used for further analysis using the Pymol Molecular Graphics System (<http://www.pymol.org>). Superposition of the PVBV model with TEV Nla-Pro structure (PDB ID: 1LVM; Phan et al., 2002) aligns 228 C-alpha atoms with RMSD of 0.43 \AA , and with TVMV protease structure (PDB ID: 3MMG; Sun et al., 2010), aligns 219 C-alpha atoms were aligned with RMSD of 1.3 \AA .

Molecular dynamics (MD) simulations were performed using GROMACS v4.0.7 (Hess et al., 2008) with OPLS-AA/L force field (Jorgensen et al., 1996). A cubic box was generated with minimum

distance of 10 Å between the solute and edge of the box. The protein models were solvated with TIP4P water model (33,653 water molecules) and neutralized with three chloride ions. Energy minimizations were performed using the steepest descent method and solvent equilibration by position-restrained dynamics of 100 ps. All the simulations were carried out under NPT conditions. Long-range electrostatic (Darden et al., 1993) and van der Waals interactions were computed with cut-off of 12 Å and 15 Å, respectively. MD simulations were performed for a time period of 30 ns and RMSDs of the trajectories with respect to the energy-minimized starting structure were calculated. Analysis of the trajectories of 30 ns simulations showed that N- and C-terminal tails of the protein show significant flexibility throughout MD simulations resulting in high RMSD values not indicative of structural changes of interest in the proteins. Thus, RMSD values of the protein backbone residues from Asn12 to Gln220 were calculated with respect to the energy-minimized structures. Backbone simulations stabilized within the first 3 ns. The RMSD values thus obtained for the wild type, S129D Nla-Pro and S129A Nla-Pro were 6.3 Å, 3.3 Å and 3.1 Å, respectively.

Supplementary materials related to this article can be found online at doi:10.1016/j.virol.2011.10.009.

Acknowledgment

We thank the Department of Biotechnology, India and Academy of Finland, Finland (Indo-Finnish grant no. 1121622), and Department of Science and Technology, India, and the Indian Institute of Science, Bangalore, for financial support. CM thanks Council for Scientific and Industrial Research (CSIR), India, for Junior & Senior Research Fellowships. We thank Prof. M. R. N. Murthy and Sagar Chittori for assistance in analyzing PVBV protease structures and for critical reading of the manuscript.

References

- Anindya, R., Savithri, H.S., 2004. Potyviral Nla proteinase: a proteinase with a novel deoxyribonuclease activity. *J. Biol. Chem.* 279 (31), 32159–32169.
- Anindya, R., Joseph, J., Gowri, T.D., Savithri, H.S., 2004. Complete genomic sequence of *Pepper vein banding virus* (PVBV): a distinct member of the genus *Potyvirus*. *Arch. Virol.* 149 (3), 625–632.
- Anindya, R., Chittori, S., Savithri, H.S., 2005. Tyrosine 66 of *Pepper vein banding virus* genome-linked protein is uridylylated by RNA-dependent RNA polymerase. *Virology* 336 (2), 154–162.
- Beauchemin, C., Boutet, N., Laliberté, J.-F., 2007. Visualization of the interaction between the precursors of VPg, the viral protein linked to the genome of Turnip mosaic virus, and the translation eukaryotic initiation factor iso 4E in planta. *J. Virol.* 81 (2), 775–782.
- Blom, N., Gammeltoft, S., Brunak, S., 1999. Sequence- and structure-based prediction of eukaryotic protein phosphorylation sites. *J. Mol. Biol.* 294 (5), 1351–1362.
- Carrington, J.C., Haldeman, R., Dolja, V.V., Restrepo-Hartwig, M.A., 1993. Internal cleavage and trans-proteolytic activities of the VPg-proteinase (Nla) of tobacco etch potyvirus in vivo. *J. Virol.* 67 (12), 6995–7000.
- Chouard, T., 2011. Structural biology: breaking the protein rules. *Nature* 471 (7337), 151–153.
- Chung, B.Y., Miller, W.A., Atkins, J.F., Firth, A.E., 2008. An overlapping essential gene in the *Potyviriidae*. *Proc. Natl. Acad. Sci. U. S. A.* 105 (15), 5897–5902.
- Darden, T., York, D., Pedersen, L., 1993. Particle mesh Ewald, An $N^{\log}(N)$ method for Ewald sums in large systems. *J. Chem. Phys.* 98, 10089–10092.
- Dougherty, W.G., Parks, T.D., 1989. Molecular genetic and biochemical evidence for the involvement of the heptapeptide cleavage sequence in determining the reaction profile at two tobacco etch virus cleavage sites in cell-free assays. *Virology* 172 (1), 145–155.
- Dougherty, W.G., Parks, T.D., 1991. Post-translational processing of the tobacco etch virus 49-kDa small nuclear inclusion polypeptide: identification of an internal cleavage site and delimitation of VPg and proteinase domains. *Virology* 183 (2), 449–456.
- Dougherty, W.G., Semler, B.L., 1993. Expression of virus-encoded proteinases: functional and structural similarities with cellular enzymes. *Microbiol. Rev.* 57 (4), 781–822.
- Ferrer-Orta, C., Arias, A., Agudo, R., Perez-Luque, R., Escarmis, C., Domingo, E., Verdager, N., 2006. The structure of a protein primer–polymerase complex in the initiation of genome replication. *EMBO J.* 25 (4), 880–888.
- Freifelder, D.M., 1982. *Physical Biochemistry*, second ed. W. H. Freeman and Company, New York.
- García, J.A., Martín, M.T., Cervera, M.T., Riechmann, J.L., 1992. Proteolytic processing of the plum pox potyvirus polyprotein by the Nla protease at a novel cleavage site. *Virology* 188 (2), 697–703.
- Grzela, R., Szolajiska, E., Ebel, C., Madern, D., Favier, A., Wojtal, I., Zagorski, W., Chroboczek, J., 2008. Virulence factor of *potato virus Y*, genome-attached terminal protein VPg, is a highly disordered protein. *J. Biol. Chem.* 283 (1), 213–221.
- Guo, D., Rajamäki, M.L., Saarma, M., Valkonen, J.P., 2001. Towards a protein interaction map of potyviruses: protein interaction matrices of two potyviruses based on the yeast two-hybrid system. *J. Gen. Virol.* 82 (4), 935–939.
- Hafren, A., Mäkinen, K., 2008. Purification of viral genome-linked protein VPg from potato virus A-infected plants reveals several post-translationally modified forms of the protein. *J. Gen. Virol.* 89 (6), 1509–1518.
- Harris, K.S., Heelien, C.U.T., Wimmer, E., 1990. Proteolytic processing in the replication of picornaviruses. *Semin. Virol.* 1, 323–333.
- Hebrard, E., Bessin, Y., Michon, T., Longhi, S., Uversky, V.N., Delalande, F., van Dorsseleer, A., Romero, P., Walter, J., Declercq, N., Fargette, D., 2009. Intrinsic disorder in Viral Proteins Genome-Linked: experimental and predictive analyses. *Virol. J.* 6, 23.
- Hess, B., Kutzner, C., van der Spoel, D., Lindahl, E., 2008. GROMACS 4: algorithms for highly efficient, load-balanced, and scalable molecular simulation. *J. Chem. Theor. Compn.* 4 (3), 435–447.
- Ivanov, K.I., Puustinen, P., Merits, A., Saarma, M., Mäkinen, K., 2001. Phosphorylation down-regulates the RNA binding function of the coat protein of potato virus A. *J. Biol. Chem.* 276 (17), 13530–13540.
- Ivanov, K.I., Puustinen, P., Gabrenaite, R., Vihinen, H., Rönstrand, L., Valmu, L., Kalkkinen, N., Mäkinen, K., 2003. Phosphorylation of the potyvirus capsid protein by protein kinase CK2 and its relevance for virus infection. *Plant Cell* 15 (9), 2124–2139.
- Jorgensen, W.L., Maxwell, D.S., Tirado-Rives, J., 1996. Development and testing of the OPLS all-atom force field on conformational energetics and properties of organic liquids. *J. Am. Chem. Soc.* 118, 11225–11236.
- Joseph, J., Savithri, H.S., 2000. Mutational analysis of the Nla protease from pepper vein banding potyvirus. *Arch. Virol.* 145 (12), 2493–2502.
- Kang, S.H., Lim, W.S., Kim, K.H., 2004. A protein interaction map of soybean mosaic virus strain G7H based on the yeast two-hybrid system. *Mol. Cells* 18 (1), 122–126.
- Kim, D.-H., Hwang, D.C., Kang, B.H., Lew, J., Han, J., Song, B.D., Choi, K.Y., 1996. Effects of internal cleavages and mutations in the C-terminal region of Nla protease of turnip mosaic potyvirus on the catalytic activity. *Virology* 226 (2), 183–190.
- Kim, D.-H., Han, J.S., Lew, J., Kim, S.S., Kang, B.H., Hwang, D.C., Jang, D.S., Kim, W., Song, B.D., Choi, K.Y., 1998. Effects of mutations in the C-terminal region of Nla protease on cis-cleavage between Nla and Nlb. *Virology* 241 (1), 94–100.
- Kim, D., Kang, B.H., Han, J.S., Choi, K.Y., 2000. Temperature and salt effects on proteolytic function of turnip mosaic potyvirus nuclear inclusion protein exhibiting a low-temperature optimum activity. *Biochim. Biophys. Acta* 1480, 29–40.
- Laskowski, R.A., Moss, D.S., Thornton, J.M., 1993. Main-chain bond lengths and bond angles in protein structures. *Mol. Biol.* 231 (4), 1049–1067.
- Leger, J., Kempf, M., Lee, G., Brandt, R., 1997. Conversion of serine to aspartate imitates phosphorylation-induced changes in the structure and function of microtubule-associated protein tau. *J. Biol. Chem.* 272 (13), 8441–8446.
- Matthews, D.A., Smith, W.W., Ferre, R.A., Condon, B., Budahazi, G.W., Sisson, J., Villafranca, E., Janson, C.A., McElroy, H.E., Gribskov, C.L., 1994. Structure of human rhinovirus 3C protease reveals a trypsin-like polypeptide fold, RNA-binding site, and means for cleaving precursor polyprotein. *Cell* 77, 761–771.
- Mavankal, G., Rhoads, R.E., 1991. In vitro cleavage at or near the N-terminus of the helper component protein in the tobacco vein mottling virus polyprotein. *Virology* 185 (2), 721–731.
- Merrifield, B., 1997. Concept and early development of solid-phase peptide synthesis. *Methods Enzymol.* 289, 3–13.
- Murray, K.E., Barton, D.J., 2003. Poliovirus CRE-dependent VPg uridylylation is required for positive-strand RNA synthesis but not for negative-strand RNA synthesis. *J. Virol.* 77 (8), 4739–4750.
- Palmenberg, A.C., 1990. Proteolytic processing of picornaviral polyprotein. *Annu. Rev. Microbiol.* 44, 603–623.
- Parks, T.D., Smith, H.A., Dougherty, W.G., 1992. Cleavage profiles of tobacco etch virus (TEV)-derived substrates mediated by precursor and processed forms of the TEV Nla proteinase. *J. Gen. Virol.* 73 (1), 149–155.
- Paul, A.V., van Boom, J.H., Filippov, D., Wimmer, E., 1998. Protein-primed RNA synthesis by purified poliovirus RNA polymerase. *Nature* 393 (6682), 280–284.
- Phan, J., Zdanov, A., Evdokimov, A.G., Tropea, J.E., Peters III, H.K., Kapust, R.B., Li, M., Wlodawer, A., Waugh, D.S., 2002. Structural basis for the substrate specificity of tobacco etch virus protease. *J. Biol. Chem.* 277 (52), 50564–50572.
- Puustinen, P., Mäkinen, K., 2004. Uridylylation of the potyvirus VPg by viral replicase Nlb correlates with the nucleotide binding capacity of VPg. *J. Biol. Chem.* 279 (37), 38103–38110.
- Puustinen, P., Rajamäki, M.L., Ivanov, K.I., Valkonen, J.P., Mäkinen, K., 2002. Detection of the potyviral genome-linked protein VPg in virions and its phosphorylation by host kinases. *J. Virol.* 76 (24), 12703–12711.
- Rajamäki, M.L., Valkonen, J.P., 2009. Control of nuclear and nucleolar localization of nuclear inclusion protein of a picorna-like Potato virus A in Nicotiana species. *Plant Cell* 21 (8), 2485–2502.
- Rantalainen, K.I., Uversky, V.N., Permi, P., Kalkkinen, N., Dunker, A.K., Mäkinen, K., 2008. Potato virus A genome-linked protein VPg is an intrinsically disordered molten globule-like protein with a hydrophobic core. *Virology* 377 (2), 280–288.
- Rantalainen, K.I., Christensen, P.A., Hafren, A., Otzen, D.E., Kalkkinen, N., Mäkinen, K., 2009. Interaction of a potyviral VPg with anionic phospholipid vesicles. *Virology* 395 (1), 114–120.

- Ravi, K.S., Joseph, J., Nagaraju, N., Prasad, S.K., Reddy, H.R., Savithri, H.S., 1997. Characterization of Pepper Vein Banding Virus from chilli pepper in India. *Plant Dis.* 81 (8), 873–876.
- Restrepo, M.A., Freed, D.D., Carrington, J.C., 1990. Nuclear transport of plant potyviral proteins. *Plant Cell* 2 (10), 987–998.
- Riechmann, J.L., Lain, S., Garcia, J.A., 1992. Highlights and prospects of potyvirus molecular biology. *J. Gen. Virol.* 73 (1), 1–16.
- Rorrer, K., Parks, T.D., Scheffler, B., Bevan, M., Dougherty, W.G., 1992. Autocatalytic activity of the tobacco etch virus Nla proteinase in viral and foreign protein sequences. *J. Gen. Virol.* 73 (4), 775–783.
- Roy Chowdhury, S., Savithri, H.S., 2011. Interaction of Sesbania Mosaic Virus Movement Protein with VPg and P10: implication to specificity of genome recognition. *PLoS One* 6 (1), e15609.
- Satheshkumar, P.S., Gayathri, P., Prasad, K., Savithri, H.S., 2005. "Natively unfolded" VPg is essential for Sesbania mosaic virus serine protease activity. *J. Biol. Chem.* 280 (34), 30291–30300.
- Schaad, M.C., Haldeman-Cahill, R., Cronin, S., Carrington, J.C., 1996. Analysis of the VPg-proteinase (Nla) encoded by tobacco etch potyvirus: effects of mutations on sub-cellular transport, proteolytic processing, and genome amplification. *J. Virol.* 70 (10), 7039–7048.
- Sun, P., Austin, B.P., Tozser, J., Waugh, D.S., 2010. Structural determinants of tobacco vein mottling virus protease substrate specificity. *Protein Sci.* 19 (11), 2240–2251.
- Tozser, J., Tropea, J.E., Cherry, S., Bagossi, P., Copeland, T.D., Wlodawer, A., Waugh, D.S., 2005. Comparison of the substrate specificity of two potyvirus proteases. *FEBS J.* 272 (2), 514–523.
- Urcuqui-Inchima, S., Haenni, A., Bernardi, F., 2001. Potyvirus proteins: a wealth of functions. *Virus Res.* 74 (1–2), 157–175.
- Wei, T., Zhang, C., Hong, J., Xiong, R., Kasschau, K.D., Zhou, X., Carrington, J.C., Wang, A., 2010. Formation of complexes at plasmodesmata for potyvirus intercellular movement is mediated by the viral protein P3N-PIPO. *PLoS Pathog.* 6, e1000962.
- Weiner, M.P., Costa, G.L., Schoettlin, W., Cline, J., Mathur, E., Bauer, J.C., 1994. Site-directed mutagenesis of double-stranded DNA by the polymerase chain reaction. *Gene* 151 (1–2), 119–123.
- Wen, R.H., Hajimorad, M.R., 2010. Mutational analysis of the putative pipo of soybean mosaic virus suggests disruption of PIPO protein impedes movement. *Virology* 400 (1), 1–7.
- Wu, S., Zhang, Y., 2007. LOMETS: a local meta-threading-server for protein structure prediction. *Nucleic Acids Res.* 35 (10), 3375–3382.